

University of Groningen

## Singlet - Singlet Annihilation in Multichromophoric Peryleneimide Dendrimers, Determined by Fluorescence Upconversion

Belder, Gino De; Schweitzer, Gerd; Jordens, Sven; Lor, Marc; Mitra, Sivaprasad; Hofkens, Johan; Feyter, Steven De; Auweraer, Mark Van der; Herrmann, Andreas; Weil, Tanja

*Published in:*  
 Chemphyschem

**IMPORTANT NOTE: You are advised to consult the publisher's version (publisher's PDF) if you wish to cite from it. Please check the document version below.**

*Document Version*  
 Publisher's PDF, also known as Version of record

*Publication date:*  
 2001

[Link to publication in University of Groningen/UMCG research database](#)

### *Citation for published version (APA):*

Belder, G. D., Schweitzer, G., Jordens, S., Lor, M., Mitra, S., Hofkens, J., Feyter, S. D., Auweraer, M. V. D., Herrmann, A., Weil, T., Müllen, K., & Schryver, F. C. D. (2001). Singlet - Singlet Annihilation in Multichromophoric Peryleneimide Dendrimers, Determined by Fluorescence Upconversion. *Chemphyschem*, 2(1), 49-55.

### **Copyright**

Other than for strictly personal use, it is not permitted to download or to forward/distribute the text or part of it without the consent of the author(s) and/or copyright holder(s), unless the work is under an open content license (like Creative Commons).

The publication may also be distributed here under the terms of Article 25fa of the Dutch Copyright Act, indicated by the "Taverne" license. More information can be found on the University of Groningen website: <https://www.rug.nl/library/open-access/self-archiving-pure/taverne-amendment>.

### **Take-down policy**

If you believe that this document breaches copyright please contact us providing details, and we will remove access to the work immediately and investigate your claim.

Downloaded from the University of Groningen/UMCG research database (Pure): <http://www.rug.nl/research/portal>. For technical reasons the number of authors shown on this cover page is limited to 10 maximum.

- [18] P. Davidson, M. Clerc, S. Ghosh, N. C. Maliszewskij, P. A. Heiney, J. Hynes, Jr., A. B. Smith, *J. Phys. II* **1995**, *5*, 249–262.  
 [19] T. Othman, M. M. Jebari, A. Gharbi, *Mol. Cryst. Liq. Cryst.* **1996**, *281*, 145–153.  
 [20] N. Derbel, T. Othman, A. Gharbi, *Liq. Cryst.* **1998**, *25*, 561–565.  
 [21] H. T. Nguyen, C. Destrade, H. Alouchi, J. P. Bideau, M. Cotrait, D. Guillon, P. Weber, J. Malthête, *Liq. Cryst.* **1993**, *15*, 435.  
 [22] S. Chandrasekhar, B. Shadashiva, K. A. Surah, *Pramana* **1977**, *9*, 471–480.  
 [23] A. M. Levelut, *J. Chem. Phys.* **1983**, *80*, 149–161.  
 [24] M. Cagnon, M. Gharbia, G. Durand, *Phys. Rev. Lett.* **1984**, *53*, 938–940.  
 [25] M. Gharbia, M. Cagnon, G. Durand, *J. Phys. Lett.* **1985**, *46*, 683.  
 [26] P. G. De Gennes, J. Prost, *The Physics of Liquid Crystals*, Oxford University Press, New York, **1993**.  
 [27] M. Gharbia, PhD thesis, Faculté des Sciences de Tunis (Tunisia), **1993**.  
 [28] J. Prost, *Liq. Cryst.* **1990**, *8*, 123–130.

Received: April 25, 2000 [Z8]

Revised: October 16, 2000

## Singlet – Singlet Annihilation in Multichromophoric Peryleneimide Dendrimers, Determined by Fluorescence Upconversion\*\*

Gino De Belder,<sup>[a]</sup> Gerd Schweitzer,<sup>[a]</sup> Sven Jordens,<sup>[a]</sup> Marc Lor,<sup>[a]</sup> Sivaprasad Mitra,<sup>[a]</sup> Johan Hofkens,<sup>[a]</sup> Steven De Feyter,<sup>[a]</sup> Mark Van der Auweraer,<sup>[a]</sup> Andreas Herrmann,<sup>[b]</sup> Tanja Weil,<sup>[b]</sup> Klaus Müllen,<sup>[b]</sup> and Frans C. De Schryver\*<sup>[a]</sup>

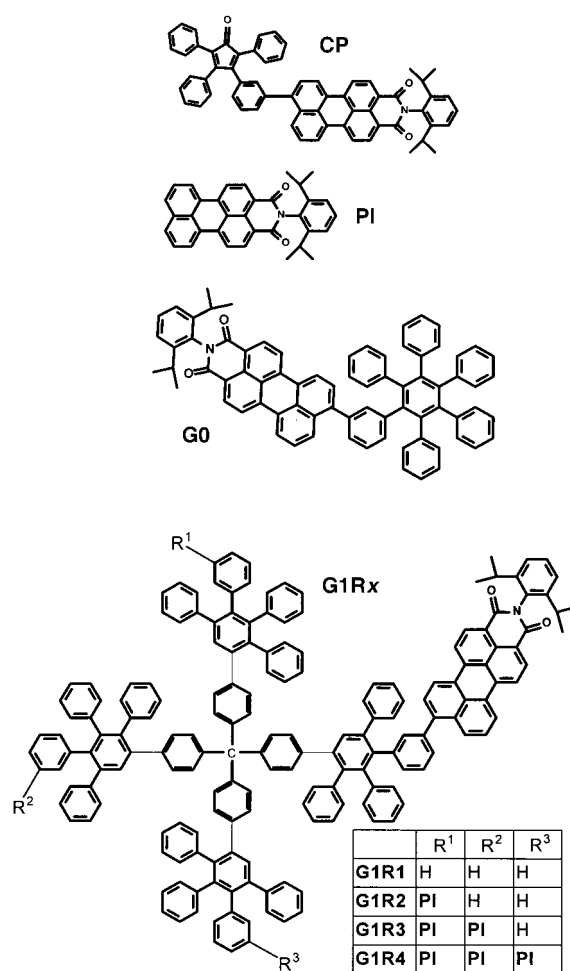
### KEYWORDS:

dendrimers · fluorescence spectroscopy · kinetics · time-resolved spectroscopy

Dendrimers are highly branched macromolecular systems whose structure can be defined on a molecular level<sup>[1,2]</sup> and, as such, have been attracting attention, not only from their synthesis,<sup>[3]</sup> but also from the point of view of their physical and chemical properties.<sup>[4–10]</sup> Within the research groups, dendrimers consisting

of a polyphenylene core and decorated with peryleneimide chromophores at the rim have been investigated by single-molecule spectroscopy<sup>[11,12]</sup> and time-resolved spectroscopy.<sup>[13–15]</sup>

However, all the studies referenced above were performed with dendrimers having a biphenyl core that leads to a conical disc-shaped structure. It was shown that the peryleneimide chromophores are distributed in different environments on the disc surface.<sup>[12]</sup> To gain better control over the distribution of chromophores and their interaction in the excited state, it is desirable to have them distributed on a spherical surface. Recently, this goal has been achieved with the synthesis of a series of first-generation peryleneimide dendrimers with a rigid tetrahedral central core, as shown in Scheme 1.<sup>[16]</sup> These



**Scheme 1.** Molecular structures of compounds: model compound **G0**, first-generation dendrimers **G1Rx** ( $x = 1–4$ ), peryleneimide **PI**, tetraphenylcyclopentadienone-bound peryleneimide **CP**.

dendrimers possess pentaphenylbenzene units and, as a result of the “interlocking” of twisted phenyl rings, are shape persistent and more closely packed, which allows a more systematic study of possible energy-transfer processes between the chromophores. Furthermore, by way of synthesis one can control the number of peryleneimide chromophores attached to the surface of the nanoparticles from one to four (**G1Rx**,  $x = 1–4$ ).<sup>[17–19]</sup>

[a] Prof. Dr. F. C. De Schryver, G. De Belder, Dr. G. Schweitzer, S. Jordens, M. Lor, Dr. S. Mitra, Dr. J. Hofkens, Dr. S. De Feyter, Prof. Dr. M. Van der Auweraer  
 Department of Chemistry  
 Katholieke Universiteit Leuven  
 Celestijnenlaan 200 F, 3001 Heverlee (Belgium)  
 E-mail: Frans.DeSchryver@Chem.KULeuven.ac.be

[b] A. Herrmann, T. Weil, Prof. Dr. K. Müllen  
 Max-Planck-Institut für Polymerforschung  
 Ackermannweg 10, 55128 Mainz (Germany)

\*\* This work was supported by the FWO, the Flemish Ministry of Education through GOA 1/96, the European Community through the TMR Sisitomas, the Bundesministerium für Education and Research of the Federal Republic of Germany, the Volkswagenstiftung and the support of DWTC (Belgium) through IUAP-IV-11. J.H. and S.D.F. thank the FWO for postdoctoral fellowships.

Many different investigations reported singlet–singlet annihilation processes in many different systems, such as pigment–protein complexes,<sup>[20–23]</sup> polymers<sup>[24]</sup> and J-aggregates.<sup>[25, 26]</sup> Herein, a very similar process is measured and reported for the first time for dendrimers decorated with multiple chromophores. For this purpose, a series of first-generation dendrimers was investigated in order to elucidate the various possible ultrafast processes including singlet–singlet annihilation which occur in mono- versus multichromophoric dendritic systems. Particular attention was paid to the excited state over the complete fluorescence emission spectrum using a time resolution of 250 fs in a time window up to 50 ps long. The photophysics of this series of compounds in the time range from 50 ps to 10 ns was studied independently with a single-photon timing setup.<sup>[27]</sup>

All compounds were investigated by steady-state absorption and emission spectroscopy; typical results are shown in Figure 1. The absorption spectra of all compounds measured are very similar. The fluorescence spectra, shown in the right of the Figure, were all recorded using an excitation wavelength of 495 nm, which is close to the absorption maximum and is the wavelength that was used in time-resolved fluorescence measurements. The spectra also do not exhibit any pronounced differences. In particular, neither a broadening nor a spectral shift was found, quite in contrast to the results reported previously<sup>[13]</sup> for another series of peryleneimide-containing dendrimers, in which the polyphenylene shell was built around a biphenyl core and the dendrimer had a higher degree of conformational mobility.

In order to reveal properties that are independent of potential chromophore–chromophore interactions, the compounds **G0** and **G1R1**, which both contain only one chromophore, were investigated in a first series of measurements. A typical

#### Editorial Advisory Board Co-Chair:

Frans C. De Schryver received his Candidate (1959), Licentiate (1961) and Doctorate (1964) in Sciences from the Katholieke Universiteit Leuven (Belgium). Following a post-doctoral Fulbright fellowship at the University of Arizona, and short stays at the Universität Stuttgart and in the Max Planck Institute for Biophysical Chemistry (Spectroscopy) in Göttingen, he returned to Leuven in 1969 to join the facility. His main research interests are in the fundamentals of photo-physical processes, such as electron or energy transfer, in organised systems and in the development of tools capable of Ångström and pico- or femtosecond resolution. He has been a Visiting Professor at the Universities of Paris-Sud, Ain Shams (Egypt) and Osaka, Academia Sinica, IBM in San José, and the Ecole Nationale Supérieure de Cachan. He is been the recipient of numerous awards including the Havinga and Porter Medals, and has acted on the boards of many of the most prestigious physical chemistry and materials journals.



[\*] Members of the Editorial Advisory Board will be introduced to the readers with their first manuscript.

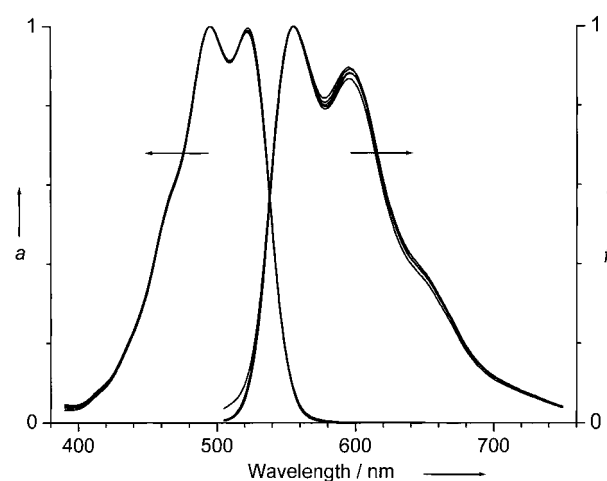


**Figure 1.** Normalised steady-state absorption (a) and emission spectra (f) of all the dendrimer molecules (**G0**, **G1R1**, **G1R2**, **G1R3** and **G1R4**). Samples for emission spectra were excited at  $\lambda = 495$  nm.

example for a decay curve of **G1R1** is depicted in Figure 2. In the top frame (Figure 2A), it can be seen that the decays are dominated by a kinetic component, the time constant thereof is much larger than this time window.<sup>[27]</sup> An expanded view of the shaded area of Figure 2A is depicted in the bottom frame

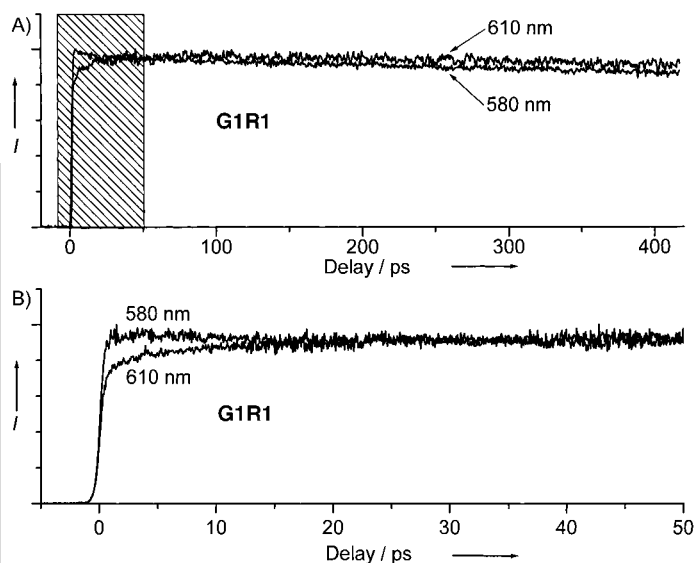


**Figure 2.** Time-resolved fluorescence intensity  $I$  of **G1R1** detected at  $\lambda = 580$  nm and 610 nm. A) The decays measured in a time window of 450 ps, the longest time window investigated. B) Expansion of the shaded region 0–50 ps in (A) (different data set).

(Figure 2B) displaying another data set from a different experiment. On the one hand, it immediately shows one or more additional short-time decay components appearing in the curves; on the other hand it exhibits pronounced differences between decays detected at 580 and 610 nm. These short decay components and their differences are in the focus of the investigation reported here.

The data analysis was performed independently for each molecule, albeit in an identical fashion. All 45 decay curves measured in all three time windows were assembled into a common data set, which was analyzed globally using a nonlinear least-squares fitting routine from a commercial software package. As part of the analysis, the data sets were also deconvoluted using information from system prompt–response measurements that were routinely recorded during each measurement session. In all cases, a sum of four exponential terms  $a_i \exp(-\tau_i)$  with time constants  $\tau_1 - \tau_4$  and amplitudes  $a_1 - a_4$  has been found necessary to fit the data sets properly, as judged by minimization of  $\chi^2$  values and visual inspection of residual plots. The longest component ( $\tau_4, a_4$ ) is in the range of a few nanoseconds and thus cannot be determined precisely in the time windows used here. Instead, the actual values were taken from measurements performed and reported independently<sup>[27]</sup> with a single-photon timing detection setup. During the fitting routine,  $\tau_4$  was fixed to 4.2 ns, however the corresponding amplitude  $a_4$  was a free parameter. It should be pointed out that the fit results were independent of this selection within the range from 3 to 6 ns.

The resulting time constants for the various compounds are summarised in Table 1. The results for  $\tau_1$  were not found to be constant throughout the spectrum and considered separately below. As can be seen in the Table, the fast component 2 exhibits

Compound	$N^{[a]}$	$\tau_1^{[b]}$ [ps]	$\tau_2$ [ps]	$\tau_3$ [ps]	$\tau_4$ [ns] <sup>[c]</sup>
<b>G1R1</b>	1	0.5–2	10	188	4.2
<b>G1R2</b>	2	0.5–2	11	180	4.2
<b>G1R3</b>	3	0.5–2	8	137	4.2
<b>G1R4</b>	4	0.5–2	7.5	83	4.2
<b>G0</b>	1	0.5–2	11.5	507	4.2
<b>PI</b>	1	0.5–2	5.5	136	4.2

[a] Number of chromophores per molecule. [b] Varies with the fluorescence detection wavelength (see text). [c] Fixed during the fit procedure (see text).

in all cases a time constant  $\tau_2$  in the order of 10 ps; the actual values range from 5.5 to 11.5 ps. Component 3 contributes at most 10% and in most cases even less to the total amplitude, however it is necessary to achieve a good fit. The actual times for this component range from 83 (**G1R4**) to 507 ps (**G0**). The largest component of the amplitude, however, is found in the nanosecond component 4 ( $\tau_4, a_4$ ) for all compounds.

In Figure 3A, the partial amplitudes for component 1 from the global analysis are shown as a function of the fluorescence detection wavelength for compounds **G1R1** and **G1R4**. In all measurements, this component showed a time constant between 0.5 and 2 ps and was found necessary to achieve a satisfactory fit. However, this component did not show a constant time value of  $\tau_1$  throughout the spectrum but, rather, increased upon an increasing fluorescence detection wavelength. This dependence is also shown in Figure 3B, which

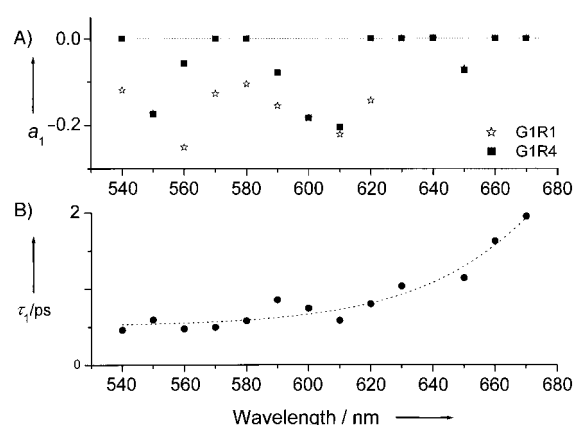


**Figure 3.** A) Dependence of the intramolecular vibrational redistribution (IVR) component amplitude  $a_1$  from the detection wavelength for **G1R1** and **G1R4**. B) The dependence of the time constant  $\tau_1$  of the IVR as a function of the detection wavelength, here shown for **G0**.

displays changes of  $\tau_1$  from 0.5 ps (540 nm detection) to 2.0 ps (at 670 nm). It should be noted, however, that the values for  $\tau_1$  are still results of global analysis and, in contrast to the other decay times, they were not linked within the common analysis of data sets of all wavelengths. Comparing the corresponding wavelength dependencies of the amplitude  $a_1$  for this component for all other compounds investigated, no pronounced differences were found: All curves seem to be similar to the ones depicted in Figure 3, that shows a negative amplitude for all wavelengths larger than 530 nm and thus corresponds to a rise term in the recorded decay. Considering these results, this component is attributed to an intramolecular vibrational redistribution (IVR) process in the electronically excited state of the chromophore.<sup>[28]</sup> A process of this kind is consistent with the properties of a kinetic component in the fluorescence decays as found here. It exhibits a negative partial amplitude at all wavelengths above 530 nm, indicating that the fluorescent state is eventually produced after completion of the IVR process.<sup>[29]</sup>

A time constant of about 1 ps has also been reported before<sup>[30–32]</sup> for various chromophores of similar size in a toluene solution. In view of the time resolution of approximately 250 fs of the setup used here, it cannot be excluded, however, that this IVR component is actually a combination of various processes resulting from the static and dynamic response of the environment of the chromophore.<sup>[33]</sup> A fast vibrational relaxation of highly excited levels of the first singlet excited state in the peryleneimide also cannot totally be excluded as a part of this component.<sup>[30]</sup>

The observation of increasing time constants for this process upon increasing detection wavelength is also in agreement with literature<sup>[29]</sup> and consistent with the attribution to an IVR process. Previously obtained results<sup>[14, 34]</sup> from ultrafast depolarisation studies of very similar dendrimers that contain identical chromophores also support this type of attribution.

Additional evidence for this assignment can be found by the comparison of emission spectra for different delay times after

excitation. As an example, the quantum flux function  $\Theta$  as calculated<sup>[14]</sup> for the compound **G1R1** from the various measured decay data are presented in Figure 4. It clearly shows a red shift of about 10 nm in the spectra in the course of time. Moreover, the complete spectral shift is finished to a large extent within the first 10 ps after excitation: Already the 5 ps spectrum almost resembles the steady-state spectrum. Thus, all the intramolecular redistribution that yields the spectral changes<sup>[35]</sup> is completed on that time scale.

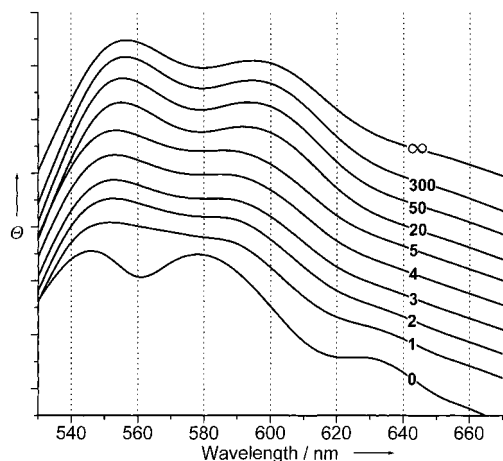


**Figure 4.** Fluorescence quantum flux  $\Theta$  for **G1R1** as calculated for different delay times (in ps, as indicated) after the excitation. The curve marked  $\infty$  is the steady-state emission spectrum.

The resulting amplitude spectra for component 2 for the **G0** and **G1R1** with time constants of 10 ps and 11.5 ps, respectively, are shown in Figure 5A. Although both of these curves result from sets of 45 decays each, which have been measured and globally analyzed independently, they appear virtually identical. Besides yielding confidence in the measurement and analysis

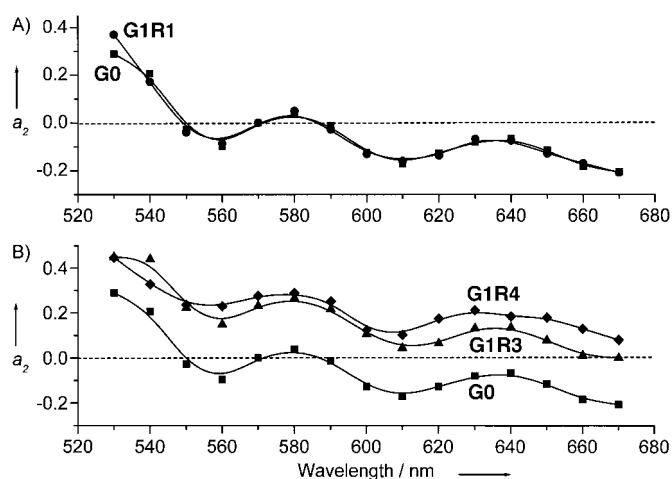


**Figure 5.** Wavelength dependence of the amplitude  $a_2$  of the 10 ps component. A) The monochromophoric compounds **G0** (■) and **G1R1** (●). B) The multichromophoric compounds **G1R3** (▲) and **G1R4** (◆) with **G0** (■) included for comparison.

procedure, this is a clear indication that the dendritic arm of the molecule does not have any effect upon the kinetics at this stage.

From the shape and the positive to negative change of this kinetic component, it is attributed to a vibrational relaxation in the electronically excited state of the peryleneimide chromophore. This process is coupled to a relaxation and reorganisation of the solvation shell around the chromophore, as the solvent molecules have to accommodate for the newly populated  $S_1$  state of the peryleneimide.<sup>[35]</sup> At fluorescence detection wavelengths close to the excitation, this will be seen as a fast decay component, whereas at longer wavelengths the fluorescence is detected from a state which first has to be populated with a time constant of about 10 ps. In the kinetic analysis, this is found as a rise term with the corresponding time constant. An identical behaviour is also found for all other investigated compounds containing only one chromophore, namely the model **G0** and **PI** in toluene (data not shown). Thus, it can be concluded that this kinetic component is related to the single chromophore itself and its interaction with the surrounding toluene (solvent) molecules.

The result of a 10 ps component and its attribution is in agreement with literature. McCarthy and Blanchard<sup>[36]</sup> used an ultrafast, stimulated transient-absorption spectroscopy setup to determine a vibrational population relaxation time constant of  $16 \pm 4$  ps for perylene in toluene solution. In many other investigations,<sup>[37–42]</sup> time constants of a few picoseconds were found and attributed to a vibrational relaxation process for various chromophores in toluene and other solvents. Moreover, in almost all experiments of sufficient time resolution, an additional, still faster, (sub-)picosecond component was found, just as reported here.

In order to investigate the influence of possible chromophore–chromophore interactions in more detail, three more sets of measurements were performed. Under otherwise identical conditions for data acquisition and analysis, compounds containing two (**G1R2**), three (**G1R3**) and four (**G1R4**) chromophores at the dendrimer rim were systematically investigated.

As expected, all the results reported above for the monochromophoric compounds could be confirmed, the corresponding values for the time constants are collected in Table 1. The only important difference was found for the 10 ps component  $\tau_2$ : Although we could not ascertain an additional time constant, the resulting amplitude spectra of the multichromophoric dendrimers were significantly different from those determined for the monochromophoric compounds. In Figure 5B, the results for **G1R3** and **G1R4** are compared to the curve determined for **G0**. It is apparent that the general shapes and wavelength dependencies are very similar, however the curves for **G1R3** and **G1R4** are shifted to larger partial amplitudes by an almost wavelength-independent offset.

Thus, to interpret these results, two different contributions,  $2a$  and  $2b$ , to this kinetic component are assumed, which are related to different processes. They both exhibit time constants  $\tau_{2a}$  and  $\tau_{2b}$  of approximately 10 ps, which are very close to each other and therefore cannot be discriminated by the global analysis, yet they can be distinguished using their respective amplitude

distributions, which are grossly different. Component  $\tau_{2a}$  is found in all dendrimers **G1R1**, **G1R2**, **G1R3** and **G1R4** as well as in the monochromophoric **G0** and **PI**. The corresponding amplitudes for all detected fluorescence wavelengths are shown in Figure 5A. This is the kinetic component which has been attributed to the vibrational relaxation process and includes solvent relaxation in the above discussion of the results for the monochromophoric compounds **G0** and **G1R1**.

Component 2, responsible for the amplitude offset, only exists in compounds containing more than one chromophore. It is superimposed on the wavelength-dependent component 2a and is almost wavelength independent and increases in amplitude with the number of chromophores (zero for one chromophore as in **G0** and **G1R1**, maximal for **G1R4**, intermediate for **G1R2** and **G1R3**).

A calculation of the photon flux available in the laser focus at the sample position yields a value of several tens of photons per chromophore per laser pulse. Moreover, by molecular modelling, the distance between the points of attachment of the chromophores is estimated to be 2.0 nm,<sup>[27]</sup> thus an interaction of two excitons existing in the molecule at the same time is likely to be the process giving rise to this kinetic component 2b. This leads to a singlet–singlet annihilation of these two excited states, to result in a first excited state and a ground state.<sup>[43]</sup> Similar processes have been reported in literature for various multichromophoric systems such as J-aggregates<sup>[25]</sup> and pigment–protein complexes,<sup>[20–23]</sup> and also been theoretically described.<sup>[43, 44]</sup>

In order to further substantiate this attribution of the component 2b, an additional series of experiments was performed. By systematic variation of the excitation power imposed onto the sample between about 20 and 350  $\mu\text{W}$ , a clear dependence of the amplitude of the 10 ps component from this parameter was observed. In Figure 6A, the decays recorded for the multichromophoric **G1R4** for two different excitation powers are shown. As this measurement was deliberately performed at a detection wavelength of 580 nm, at which the amplitude of component 2a is close to zero (compare with Figure 5A), this clearly visible dependence is solely attributed to component 2b. The dependence of the partial amplitude  $a_2$  of this kinetic component on the laser power impinging on **G1R4** is depicted in Figure 7, which reveals typical dependencies found for annihilation processes.<sup>[44]</sup>

Repeating this procedure for a similar series but with detection at 620 nm, the results differ (Figure 6B). Here, at high power excitation, a *decay component* indicative of component 2b is found, which becomes a *rise term* with the same time constant at low power excitation and thus shows only component 2a. Again, the corresponding power plot is shown in Figure 7. In this case, the amplitude  $a_2$  ranges from negative values at low power excitation to positive values for high laser excitation power. With respect to the various amplitudes as shown in Figure 5, this behaviour is as expected and an additional strong support for the assumption that component 2, that results from the global analysis, is in fact a combination of two processes 2a and 2b, as described above.

In order to cross check these findings, a similar power series has also been performed for monochromophoric **G1R1**. The

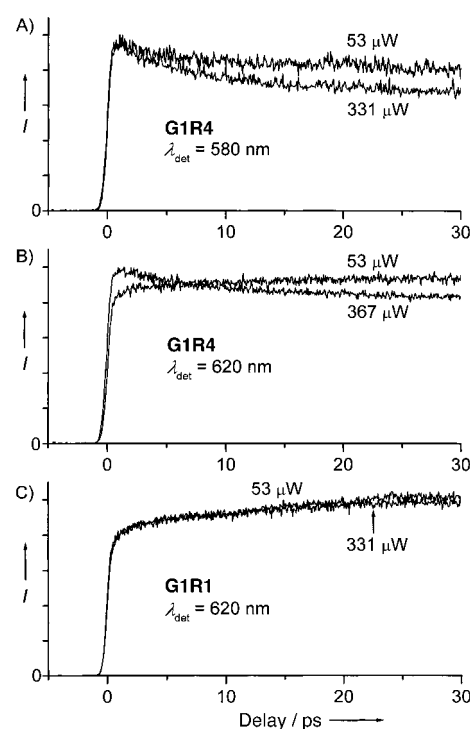


**Figure 6.** Comparison of the time resolved fluorescence intensity  $I$  recorded at low and high excitation power, as indicated. A) Multichromophoric compound **G1R4**, detected at 580 nm, B) multichromophoric compound **G1R4**, detected at 620 nm, C) monochromophoric compound **G1R1**, detected at 620 nm.

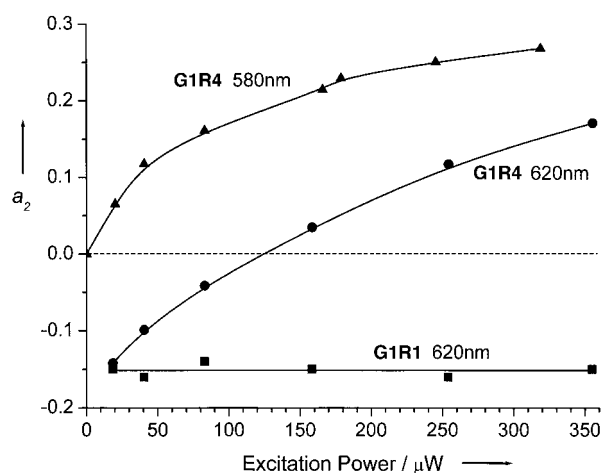


**Figure 7.** Dependence of the partial amplitude  $a_2$  of the 10 ps component from the laser excitation power for monochromophoric **G1R1** (■) and the multichromophoric **G1R4** (detected at 580 (▲) and 620 (●) nm).

results, shown in Figure 6C, are as expected: In contrast to the multichromophoric **G1R4** measured at this wavelength (Figure 6B), there is no detectable power dependence within the measured range. Thus, at all excitation intensities, the partial amplitudes  $a_2$  are constant (see Figure 7), which is a clear indication that, in this monochromophoric compound, component 2b is nonexistent.

The kinetic component 3 with a corresponding time constant  $\tau_3$  in the order of 100 ps is found in all data sets yet at a relatively low partial amplitude  $a_3$ . By performing an additional measurement series that systematically varies the concentration of the dendrimers in the toluene solution, it was the only one that showed any change (data not shown). It is thus attributed in part to an intermolecular process and not discussed here further. It should be noted, however, that this component is already seen with a low partial amplitude at the lowest compound concentration experimentally accessible for fluorescence upconversion measurements.

Component 4 used in the analysis with a time constant of 4.2 ns and its amplitude spectra as shown in the Figure 4 is clearly attributed to the fluorescence lifetime of the peryleneimide chromophore and dealt with in detail in a separate publication.<sup>[27]</sup>

To conclude, by systematic variation of the number of chromophores in a first-generation peryleneimide dendrimer, a number of kinetic processes could be found and assigned. In all compounds, an intramolecular vibrational redistribution process with a time constant of about 1 ps is apparent. All compounds also exhibit a 10 ps kinetic component, which is attributed to a vibrational relaxation process in the electronically excited state. In all compounds that contain more than one chromophore, an additional competitive 10 ps process is observed. This process is attributed to a singlet–singlet annihilation occurring in the multichromophoric dendritic systems. This assignment was verified by various power-dependent excitation measurement series.

## Experimental Section

In this study, six different compounds were investigated. Four are derivatives of a first-generation dendrimer with a tetraphenylmethane core (**G1**) decorated with one (**G1R1**), two (**G1R2**), three (**G1R3**) and four (**G1R4**) peryleneimide chromophores on the rim. The synthesis of these compounds utilised the tetraphenylcyclopentadienone **CP** which carries the peryleneimide chromophore.<sup>[19]</sup> While **G1R4** was made via Diels–Alder cycloaddition of **CP** to a core molecule with four ethynyl functionalities, the “desymmetrised” species **G1R1**, **G1R2** and **G1R3** require a novel approach which will appear elsewhere.<sup>[16]</sup> The additional two compounds, a peryleneimide with one hexaphenylbenzene moiety attached (**G0**) and the pure peryleneimide chromophore itself (**PI**), are reference compounds of only one chromophore in order to distinguish the various kinetic components.

All measurements were performed at room temperature in 1 mm optical path length cuvettes under magic angle polarization conditions. All compounds were dissolved in toluene at a concentration that yielded an absorption of about  $0.4 \text{ mm}^{-1}$  at 495 nm.

The laser system has previously been described in detail.<sup>[45]</sup> In brief, a Nd:YVO<sub>4</sub> laser (Millennia V, Spectra Physics) is used to pump a Ti:sapphire laser (Tsunami, Spectra Physics). Its output seeds a regenerative amplifier (RGA; Spitfire, Spectra Physics). The output of the RGA (1 mJ, 100 fs, 800 nm) is split in two equal parts, one of which is used to pump an optical parametric generator/amplifier (OPA-800, Spectra Physics). The output wavelength range of the OPA

is extended by harmonic generation using one or two  $\beta$ -BaB<sub>2</sub>O<sub>4</sub> (BBO) crystals, thus the range 300–900 nm is accessible.

The setup used for the detection of the fluorescence upconversion signal has also been described.<sup>[14]</sup> Briefly, the fluorescence light emitted from the sample is collected and sent to a LiB<sub>3</sub>O<sub>5</sub> (LBO) crystal, in which the sum frequency of this light and a gate pulse (about 400  $\mu\text{J}$  at 800 nm) derived from the RGA is generated. The time-resolved traces are then collected by detecting this sum-frequency light while changing the relative delay of the gate pulse versus the sample excitation time. By detection of scattered light under otherwise typical conditions, the prompt response of this setup was 250 fs. This value was used in the analysis of all measurements for deconvolution of the data sets.

For all measurements, the excitation wavelength was kept constant at 495 nm. Except for the series checking the excitation power dependence (see below), all compounds were illuminated with an excitation energy of about 350 nJ. Each measurement consisted of 1024 delay positions, at each of which the fluorescence signal, the excitation laser intensity and the gate pulse intensity were recorded over an average of five seconds, thus resulting in a measurement time of about 5000 s per delay scan. By taking a steady-state absorption spectrum before and after each set of measurements, the sample integrity under these conditions was verified.

To capture all kinetic components potentially present in the excited-state dynamics as precisely as possible, a measurement as described above was then repeated using three different channel widths for the detection, resulting in total time windows of 6.7, 50 and 450 ps, respectively, for all 1024 measured channels. This set of three measurements was performed for each compound throughout its complete emission spectrum, thus resulting in 15 different fluorescence detection wavelengths from 530 to 670 nm at intervals of 10 nm.

In order to investigate possible multiphoton processes, an additional series of measurements was performed varying the laser energy exciting the compound in a systematic way while keeping all other conditions constant. This was done in a range from 350 (maximum laser output available) to 20 nJ, which was close to the detection limit, as one measurement under these conditions had to last about 20 hours to yield data sets which could still be analyzed.

Finally, in a separate measurement series, the concentration dependence of the dendrimers between  $10^{-4}$  and  $10^{-5}$  molar was investigated. In order to do this, the standard concentration used in all other sets was reduced by a factor of ten for another measurement sequence.

- [1] S. Toppet, K.R. Gopidas, A.R. Leheny, G. Caminati, N.J. Turro, D.A. Tomalia, *J. Am. Chem. Soc.* **1991**, *113*, 7335.
- [2] R. Duan, L. Miller, D.A. Tomalia, *J. Am. Chem. Soc.* **1995**, *117*, 10783.
- [3] C. J. Hawker, J. M. Frechet in *Step-Growth Polymers for High Performance Materials: New Synthetic Methods* (Eds.: J.L. Hendrick, G. Lanzani), American Chemical Society, New York, **1996**, p. 132.
- [4] K. A. Aoi, K. Itah, M. Okada, *Macromolecules* **1995**, *28*, 5391.
- [5] A. Archut, F. Vogtle, *Chem. Soc. Rev.* **1998**, *27*, 233.
- [6] S. C. Zimmerman, F. W. Zeng, D. E. C. Reichert, S. V. Kolotuchin, *Science* **1996**, *271*, 1095.
- [7] J. M. Frechet, *Science* **1994**, *263*, 1710.
- [8] D. A. Tomalia, *Top. Curr. Chem.* **1993**, *165*, 193.
- [9] F. Morgenroth, C. Kubel, K. Mullen, *J. Mater. Chem.* **1997**, *7*, 1207.
- [10] E. K. L. Yeow, K. P. Ghiggino, J. N. H. Reek, M. J. Crossley, A. W. Bosman, A. P. H. J. Schenning, E. W. Meijer, *J. Phys. Chem. B* **2000**, *104*, 2596.
- [11] T. Gensch, J. Hofkens, A. Herrmann, K. Tsuda, W. Verheijen, T. Vosch, T. Christ, T. Basché, K. Mullen, F. C. De Schryver, *Angew. Chem.* **1999**, *111*, 3970; *Angew. Chem. Int. Ed.* **1999**, *38*, 3752.

- [12] J. Hofkens, M. Maus, T. Gensch, T. Vosch, M. Cotlet, F. Köhn, A. Herrmann, K. Müllen, F. C. De Schryver, *J. Am. Chem. Soc.* **2000**, *122*, 9278.
- [13] J. Hofkens, L. Latterini, G. De Belder, T. Gensch, M. Maus, T. Vosch, Y. Karni, G. Schweitzer, F. C. De Schryver, A. Herrmann, K. Mullen, *Chem. Phys. Lett.* **1999**, *304*, 1.
- [14] Y. Karni, S. Jordens, G. De Belder, G. Schweitzer, J. Hofkens, T. Gensch, M. Maus, F. C. De Schryver, A. Herrmann, K. Mullen, *Chem. Phys. Lett.* **1999**, *310*, 73.
- [15] Y. Karni, S. Jordens, G. De Belder, J. Hofkens, G. Schweitzer, F. C. De Schryver, *J. Phys. Chem. B* **1999**, *103*, 9378.
- [16] T. Weil, U. M. Wiesler, A. Herrmann, K. Mullen, *J. Am. Chem. Soc.* **2000**, submitted.
- [17] F. Morgenroth, E. Reuther, K. Mullen, *Angew. Chem.* **1997**, *109*, 647; *Angew. Chem. Int. Ed. Engl.* **1997**, *36*, 631.
- [18] F. Morgenroth, K. Mullen, *Tetrahedron* **1997**, *53*, 15349.
- [19] F. Morgenroth, C. Kubel, M. Muller, U. M. Wiesler, A. J. Berresheim, M. Wagner, K. Mullen, *Carbon* **1998**, *36*, 833.
- [20] V. Gulbinas, L. Valkunas, D. Kuciauskas, E. Katilius, V. Liuliola, W. L. Zhou, R. E. Blankenship, *J. Phys. Chem.* **1996**, *100*, 17950.
- [21] L. Valkunas, V. Gulbinas, *Photochem. Photobiol.* **1997**, *66*, 628.
- [22] V. Barzda, G. Garab, V. Gulbinas, L. Valkunas, *Biochim. Biophys. Acta Bioenerg.* **1996**, *1273*, 231.
- [23] W. H. J. Westerhuis, M. Vos, R. van Grondelle, J. Amesz, R. A. Niederman, *Biochim. Biophys. Acta Bioenerg.* **1998**, *1366*, 317.
- [24] A. Ruseckas, M. Theander, L. Valkunas, M. R. Andersson, O. Inganas, V. Sundstrom, *J. Lumin.* **1998**, *76–77*, 474.
- [25] V. Sundstrom, T. Gillbro, R. A. Gadonas, A. Piskarskas, *J. Phys. Chem.* **1988**, *89*, 2754.
- [26] I. G. Scheblykin, O. P. Varnavsky, M. M. Bataiev, O. Sliusarenko, M. Van der Auweraer, A. G. Vitukhnovsky, *Chem. Phys. Lett.* **1998**, *298*, 341.
- [27] M. Maus, S. Mitra, M. Lor, T. Weil, J. Hofkens, K. Mullen, F. C. De Schryver, submitted.
- [28] D. J. Nesbitt, R. W. Field, *J. Phys. Chem.* **1996**, *100*, 12735.
- [29] J. S. Baskin, L. Banares, S. Pedersen, A. H. Zewail, *J. Phys. Chem.* **1996**, *100*, 11920.
- [30] T. Nakabayashi, H. Okamoto, M. Tasumi, *J. Phys. Chem. A* **1997**, *101*, 3494.
- [31] I. V. Rubtsov, K. Yoshihara, *J. Phys. Chem. A* **1999**, *103*, 10202.
- [32] H. Zhang, A. M. Jonkman, P. van der Meulen, M. Glasbeek, *Chem. Phys. Lett.* **2000**, *224*, 551.
- [33] M. L. Horng, J. A. Gardecki, A. Papazyan, M. Maroncelli, *J. Phys. Chem.* **1995**, *99*, 17311.
- [34] G. Schweitzer, G. De Belder, S. Jordens, Y. Karni, F. C. De Schryver, unpublished results.
- [35] R. M. Stratton, M. Maroncelli, *J. Phys. Chem.* **1996**, *100*, 12981.
- [36] P. K. McCarthy, G. J. Blanchard, *J. Phys. Chem.* **1996**, *100*, 14592.
- [37] T. Gustavsson, G. Baldacchino, J. C. Mialocq, S. Reekmans, *Chem. Phys. Lett.* **1995**, *236*, 587.
- [38] W. Jarzaba, G. C. Walker, A. E. Johnson, M. A. Kahlow, P. F. Barbara, *J. Phys. Chem.* **1998**, *92*, 7039.
- [39] Y. Kimura, J. C. Alfano, P. K. Walhout, P. F. Barbara, *J. Phys. Chem.* **1994**, *98*, 3450.
- [40] L. Reynolds, J. A. Gardecki, S. J. V. Frankland, M. L. Horng, M. Maroncelli, *J. Phys. Chem.* **1996**, *100*, 10337.
- [41] P. Changenet, P. Plaza, M. M. Martin, Y. H. Meyer, *J. Phys. Chem. A* **1997**, *101*, 8186.
- [42] P. Changenet, H. Zhang, M. J. van der Meer, K. J. Hellingwerf, M. Glasbeek, *Chem. Phys. Lett.* **1998**, *282*, 276.
- [43] R. D. Harcourt, K. P. Ghiggino, G. D. Scholes, R. P. Steer, *J. Chem. Phys.* **1998**, *109*, 1310.
- [44] G. Paillotin, C. E. Swenberg, J. Breton, N. E. Geacintov, *Biophys. J.* **1979**, *25*, 513.
- [45] G. Schweitzer, L. Xu, B. Craig, F. C. De Schryver, *Opt. Commun.* **1997**, *142*, 283.

Received: July 31, 2000 [Z80]

## Effects of Oxidation on the Nanoscale Mechanisms of Crack Formation in Aluminum\*\*

Emily A. A. Jarvis,<sup>[a]</sup> Robin L. Hayes,<sup>[a]</sup> and Emily A. Carter<sup>\*\*[a]</sup>

### KEYWORDS:

aluminum · cracking · density functional calculations · materials science · surfaces

Materials failure, in the form of cracking, is a phenomenon of fundamental scientific interest and one that impacts a variety of applications spanning a wide range of fields, particularly those of materials science and engineering. Experiments have investigated extensively the macroscopic properties associated with cracking within homogeneous materials as well as at interfaces between dissimilar materials. Likewise, theoretical modeling via engineering finite-element approaches<sup>[1]</sup> and molecular dynamics simulations with empirical embedded-atom potentials<sup>[2, 3]</sup> have provided some insight into cracking mechanisms. Nevertheless, these models rely on inherent assumptions concerning interatomic and/or bulk behavior, a drawback in instances where fundamental atomic interactions are poorly understood or improperly characterized by overly simplified model potentials. A comprehensive study incorporating a first principles approach at the atomic scale and effectively linking this information to the macroscopic scale poses an array of challenges, implementational and otherwise. To date, these difficulties and the computational expense associated with first principles calculations have generally motivated employing empirical assumptions to treat mechanics of the smallest length-scale regime. Resorting to empirical models limits the chemistry that may be accounted for. Accordingly, despite widespread scientific interest in the cracking phenomenon, aspects of the microscopic failure mechanisms remain largely a mystery. Herein, we investigate some aspects of the atomic-level properties which lead to chemically induced crack formation within a simple model. Finding methods to smoothly and effectively couple microscopic to macroscopic modeling is an active area of research<sup>[4, 5]</sup> and will provide much-needed insight into a complete mechanism for chemically induced cracking.

Aluminum is an important engineering material used in a variety of applications; to understand its behavior under stress is essential. Under ambient conditions, a self-limiting oxide layer forms on the aluminum surface and protects the underlying metal from further oxidation. This, in addition to their light

[a] Prof. E. A. Carter, E. A. A. Jarvis, R. L. Hayes  
Department of Chemistry and Biochemistry  
University of California, Los Angeles  
Los Angeles, CA 90095-1569 (USA)  
Fax: (+1) 310-267-0319  
E-mail: eac@chem.ucla.edu

[\*\*] We are grateful to the US Air Force Office of Scientific Research through the US Department of Defense MURI program for support of this work.